INSTITUTE OF PLASMA PHYSICS
CZECHOSLOVAK ACADEMY OF SCIENCES

First Results from sin - cos Reflectometer on CASTOR

Kletečka P.

RESEARCH REPORT

IPPCZ - 347 February 1995

POD VODÁRENSKOU VĚŽÍ 4, 180 69 PRAGUE 8
CZECHOSLOVAKIA

First Results from sin-cos Reflectometer on CASTOR

Kletečka P.

IPPCZ-347

February 1995

First Results from sin-cos Reflectometer on CASTOR

Kletečka P.
Institute of Plasma Physics, Za Slovankou 3, 18200 Prague 8
Czech Republic

Introduction

A homodyne reflectometer with sin-cosin detection system, operating in the O-mode. has been installed and operated on CASTOR tokamak for the study of density fluctuations[1]. The reflectometer can be used in the frequency range 8-18 GHz. First results was obtained on fixed frequencies 8.5 GHz and 10.26 GHz in O-mode polarization.

Homodyne Reflectometer with sin-cosin Phase Detection System

The reflectometer with sin-cosin phase detection is very suitable diagnostic for measurement of density fluctuations. The Fig.1 shows schematically reflectometer built for CASTOR. As a generator a gunn oscilator with power 200mW is used. The gunn oscilator is operated on two fixed frequencies 8.5 GHz and 10.26 GHz.

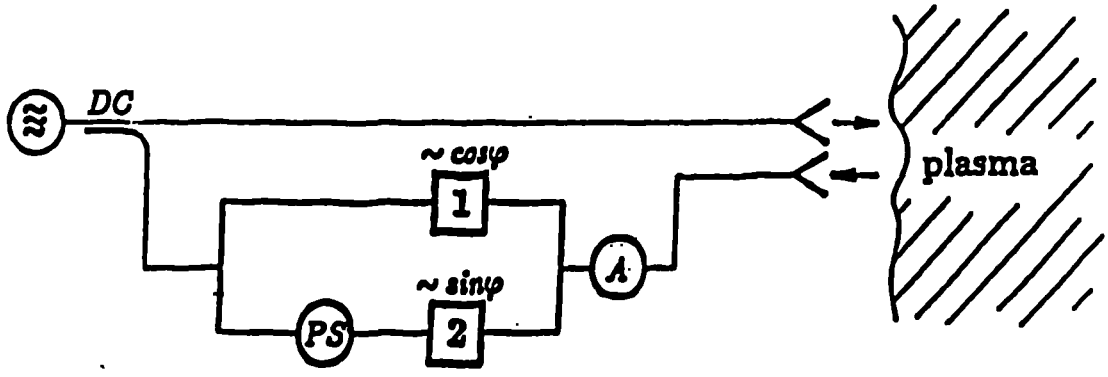

Figure 1: Scheme of the sin-cosin reflectometer; DC-directional coupler -10dB, A-attenuator, PS-phase shifter, 1 and 2 are mixing detectors.

The antenna system consists of two rectangular horns. The Fig.2 shows the dimensions of antenna system. The horns are located on the equatorial midplane with an angle of 10° relative to one another with their apertures located at R=0.505m (R_0=0.4m and a=0.01m) so that their sightlines cross at r/a=0.3. The antenna system is located inside the tokamak horizontal port with the width 80mm from low field side. The wavequide teflon windows are used as a vacuum interface.

The gain of horns is not high, because the dimensions of used antenna system are fo. frequency range 8-18 GHz relatively small due to the small dimensions of the vacuum port. On the other hand the dual antenna arrangement greatly reduces the effects of internal reflections in the waveguide system as compared to a single antenna system[2].

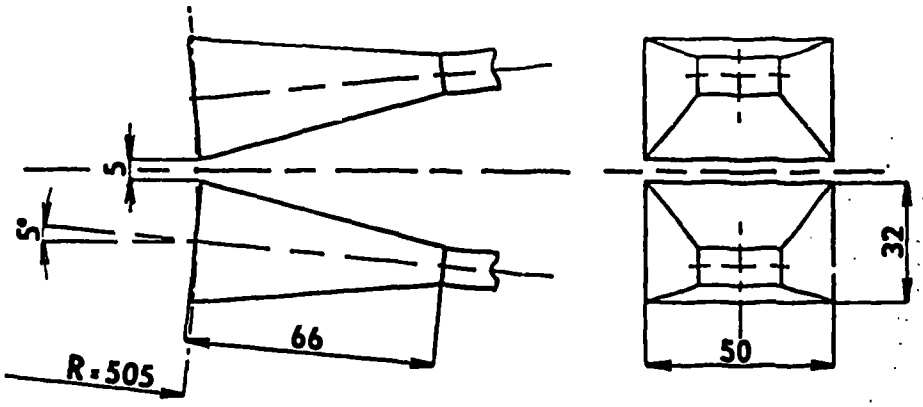

Figure 2: The antenna system dimensions.

The sin-cosin phase detection system is suitable for the measurement of plasma density fluctuations. A 90° phase delay is inserted between the two detectors. The large voltage offset in output signal is removed electronically (AC coupling) or digitally (in software)[1].

CASTOR Operational Regime.

Tokamak CASTOR [2] is small device with R/a=0.4/0.1, toroidal magnetic field $B_{t,v} \leq 1.5$T, plasma current $I_p \leq 30$kA, plasma average density $\bar{n} \leq 2 \times 10^{19} m^{-3}$ and pulse duration $\tau \leq 40$ms. The density range which can be studied on CASTOR with 8 to 18 GHz reflectometer is $(0.8\text{-}4)\times 10^{18} m^{-3}$ for O mode operation.

Spectral Analysis of Fluctuation Data.

The analysis of fluctuation data, known as spectral analysis, is primarily carried out in the frequency domain, that is, the array of phase fluctuation data vs time is tranformed into the frequency domain to obtain the fluctuation frequency spectra. In this way, the amplitude of each frequency component in the spectrum can be observed, which allows the signal analysis to concetrate on the dominant fluctuations. A transient recorder with a sampling frequency f_s=2MHz and memory 4kB for each channel has been used for data collection. The sampling interval is then $\Delta t = 1/f_s$, and the time length of the digitized signal is $T = n_T \Delta t$. Low-pass filtering is performed to eliminate aliasing of the data. Aliasing of the data occurs when fluctuations with frequencies greater than the Nyquist frequency ($f_N = f_s/2$)are present in the input signal. The time length of the digitized signal T is divided into four temporal window $\Delta T = N \Delta t$, where $N = n_T/4 = 1024$ data points. Thus, the transformation results in a time averaging over ΔT.

The frequency resolution of the transformed signal is determined by the number of data points N over which the Fourier transform is calculated and the leakage effect associated with windowing the data. The problem of leakage is inherent in the fourier analysis of any finite record. The record has been formed by looking at the actual signal for a period of T microseconds and by neglecting everything that happened before or after this period. This is equivalent to multiplying the continuous signal by a rectangular data window. When the transformation to the frequency domain is made, the effect of the rectangular data window is a function with an amplitude of the form (sin x)/x centered at the frequency of each waveform in the signal. This ampplitude function has a series of sidelobes (spurious peaks), which give false contributions to the amplitude of the waveforms at other frequencies. This sidelobe contribution is the leakage effect. The leakage problem is minimized by aplyiyng a data window, other than a rectangular window, to the time series signal, which has lower sidelobes when transformed to the frequency domain. This windowing function simply provides a smoother beginning and ending to the record to minimize the sidelobe production [4].

The frequency resolution Δf is then given by the ratio of the spectrum width or sampling frequency f_s to number of intervals used in the the transform, $\Delta f = f_s/N$, and so to obtain better frequency resolution, a longer signal and so more time averaging must be used. The transformed signal can be used one temporal window at a time or $n_w = n_T/N$ windows can be averaged to obtain the average spectra, where $n_w \leq n_T/N$ and is a whole number. Overlapping windows with $n_w = 2n_T/N - 1$ (obtained by stepping N/2 records for each realization) can be used to increase the number of windows being averaged over to improve the statistical accuracy of the spectra.

Discrete Fourier Transform

The discrete Fourier transform (DFT) pair that applies sampled versions of the continuous signals s(t) and S(f) is [5]

$$X(f_j) = \frac{1}{N}\sum_{t_k=0}^{N-1} x(t_k) exp\frac{-i2\pi f_j t_k}{N}$$

$$x(t_k) = \sum_{f_j=0}^{N-1} X(f_j) exp\frac{i2\pi f_j t_k}{N}$$

for f_j=0, 1..... N-1 and t_k=0, 1..... N-1. $X(f_j)$ and $x(t_k)$ simply represent discrete samples of the continuous waveforms S(f) and s(t). Note that $X(f_j)$ and $x(t_k)$ are, in general, complex series. Although most of the properties of the continuous Fourier transform are retained, some differences do results from the constraint that the DFT must operate on sampled waveforms defined over finite intervals.

When $x(t_k)$ is real, the real part of $X(f_j)$ is symmetric about the folding frequency f_f where $f_f = f_s/2$, and the imaginary part is antisymmetric.

This means that the Fourier coefficient between 0 and $\frac{N}{2}$-1 can be viewed as the positive frequency (real) components of the signal, while the coefficients between -N/2 and N-1 can be viewed as the negative frequency harmonics between -N/2 and 0. When $x(t_k)$ is real, the negative frequency harmonics are simply a mirror image of the real components between N/2 and N-1 represent the frequency of waves traveling in the reverse direction.

Fast Fourier Transform.

The FFT is the primary digital method of transforming signals from the time domain to the frequency domain. The FFT rapidly computes a good approximation of the DFT for a finite-duration sampled signal. The efficient application of the FFT requires that the window length contain $N = 2^p = 1024$ records, where p is a rational number. The data signal is then divided up into $n_\omega = 4$ realizations. Each realization is multiplyed by a window of length N and processed through the FFT procedure to obtain the DFT of the record. The output record is complex, having an amplitude and phase. The auto-power spectral density (APSD) or power spectrum of the original function is obtained by squaring the complex output record, $APSD = X(f_j)^2 = X(f_j)X(fj)^*$ where $X(f_j)^*$ is the complex conjugate.

Cross (Auto)-Correlation Analysis

The correlation of two signals provides the similar component present in both signals as the output. The correlation integral for two signals x(t) and y(t) is defined as

$$c_{xy}(\tau) = \lim_{T-\infty} \frac{1}{T} \int_0^T x(t)y(t+\tau)\,dt$$

where c_{xy} is precisely the cross-correlation function representing the total correlation between x(t) and y(t), and τ in $y(t+\tau)$ represents a time delay between the two signals. For $\tau = 0$, the equal-time cross-correletion function is obtained. The auto-correlation function is the special case of x=y. For discrete sampled signals, the cross-correlation function of $x(t_k)$ and $y(t_k)$ is defined as

$$c_{xy}(\tau_k) = \frac{1}{N} \sum_{t=0}^{N-1} x(t)y(t+\tau_k)$$

The easiest way to obtain the cross-correlation function is via the frequency domain and the FFT. If $X(f_j)$ and $Y(f_j)$ represent the DFTs of $x(t_k)$ and $y(t_k)$, respectively, then the frequency domain cross-correlation function can be obtained from

$$C_{xy}(f_j X(f_j Y(f_j)$$

where $C_{xy}(f_j)$ is the DFT of $c_{xy}(\tau_k)$ and is called the cross-power spectra density (CPSD). If $x(t_k) = y(t_k)$, the APSD will be obtained. Since the cross-correlation function is complex, it contains the amplitude and phase of the coherent parts of the two initial signals.

The amplitude is known as the cross-spectral amplitude, while the phase is knonw as the cross-spectral phase and represents the phase delay between the two signals for each f_j component. The phase has a range of $-\pi \rightarrow \pi$.

ASTOR Reflectometer Signal/Data Analysis

Fig.2 shows the basic layout of the emitter follower and data acquisition (DAQ) system for CASTOR reflectometer.

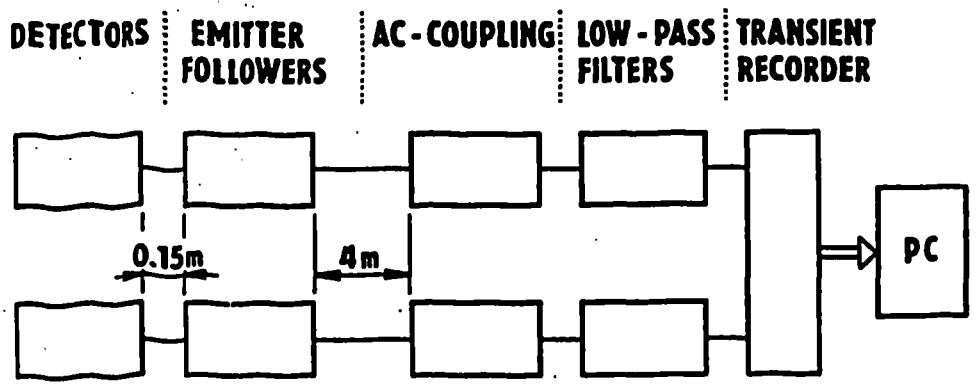

igure 2: A block diagram of the detection, emitter follower and data acquisition system used on ASTOR reflectometer.

Due to the long coaxial cable (10m) to transient recorder the detectors were connected to the emitter followers. The maximum sampling frequency of the digitizer is 2MHz so the anti-aliasing low-pass filter cutoff frequency is never greater than half system bandwidth. The voltage offset in output signal is removed ac coupling (capacitor). The mixing detectors have not the same calibration curve. The output signals from detectors are necessary to multiply by calibration curves of detectors to obtaining the right power level of signal.

lodeling of the Reflectometer Data

The simple model of reflectometer data was used. The cutoff layer position and phase delay were computed from the measured average density (from interferometer). We supposed parabolical density profile , which is not change during discharge.

The phase delay of a wave propagating in the plasma up to the position of the critical density layer is given by

$$\varphi_{pl} = \frac{\omega}{c}\int_{R_c}^{R_{ant}} \sqrt{(1 - \frac{\omega_{pe}^2}{\omega^2})}\, dR - \frac{\pi}{2}$$

c....the velocity of light
ω_{pe}....the electron plasma frequency
R_{ant}....the posititon of the anntena outside the plasma
R_c....the position of the reflection layer in the plasma
All positions are relative to the axis of rotational symmetry of the tokamak.

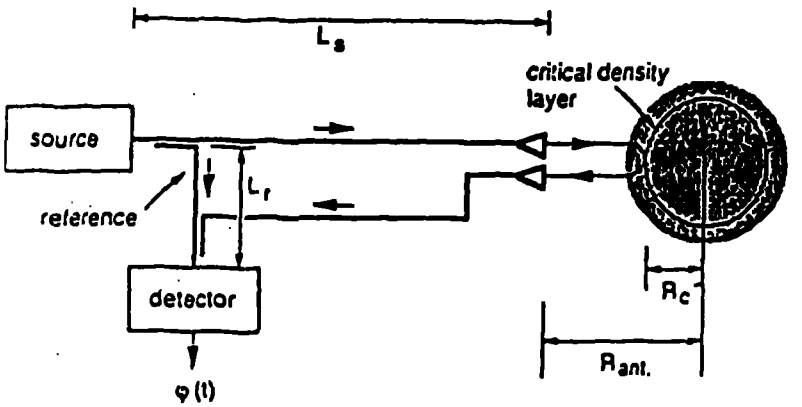

Figure 4. A schematic representation of the reflectometer

The Fig.5a and Fig.5b show time evolution of the phase delay (phase) and the cutoff layer position (dista) from the measured electron density (dens).

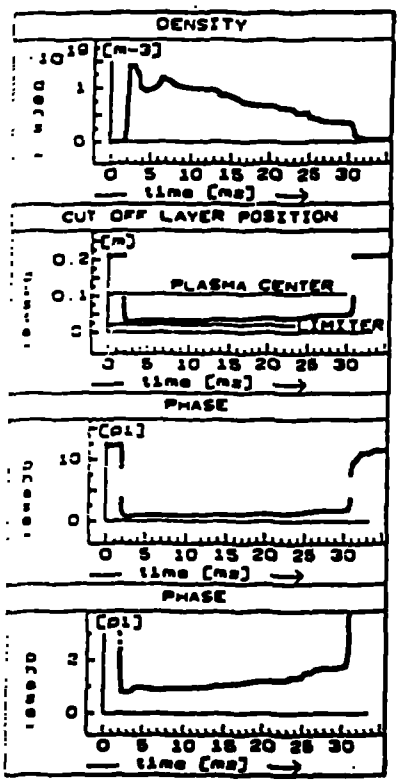

Fig.5a. Modeling data

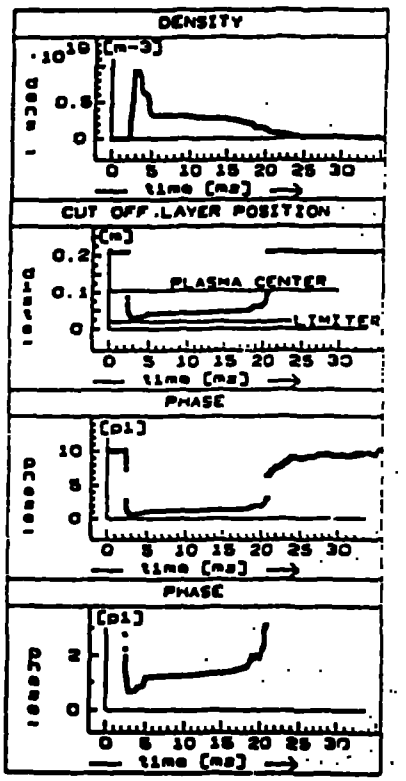

Fig.5b. Modeling data

The cutoff layer position ($R_{wall} - R_c$) and the phase delay are shown for fixed frequencies 8.5GHz in Fig.5a and 10.26GHz in Fig.5b Figures 5a and 5b show that the probing signal is reflected on plasma periphery.

Experimental Results

The CASTOR reflectometer has operated in ohmical regime with electron densities $(0.3 - 1) \times 10^{19} m^{-3}$ in plasma center on the two fixed frequencies 8.5GHz and 10.26GHz. This arrangement of operation allows to measure the fluctuations on the plasma periphery. The phase delay signals were obtained from the raw reflectometer data [1]. Using the auto-correlation and FTT analysis techniques were obtained some frequency spectra and the autocorrelation parameter $\Delta\tau$. Fig.6 shows the typical auto-correlation function of the phase delay signal of. The curve was computed using 10^3 samples.

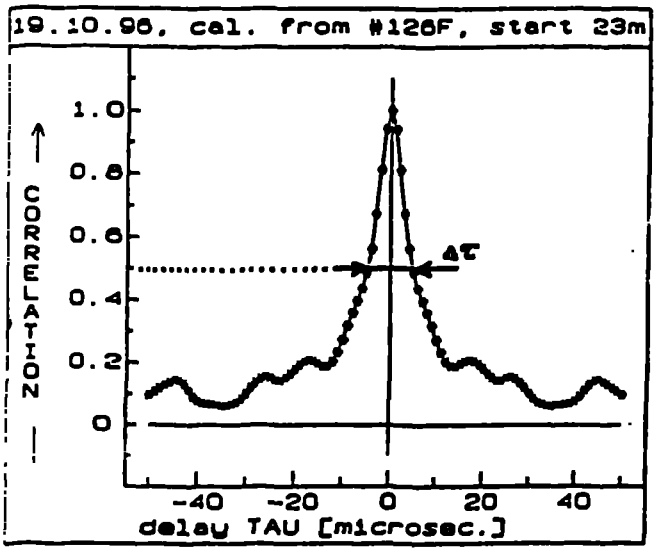

Figure 6: A typical auto-correlation function of the phase signal starting from 23ms of discharge.

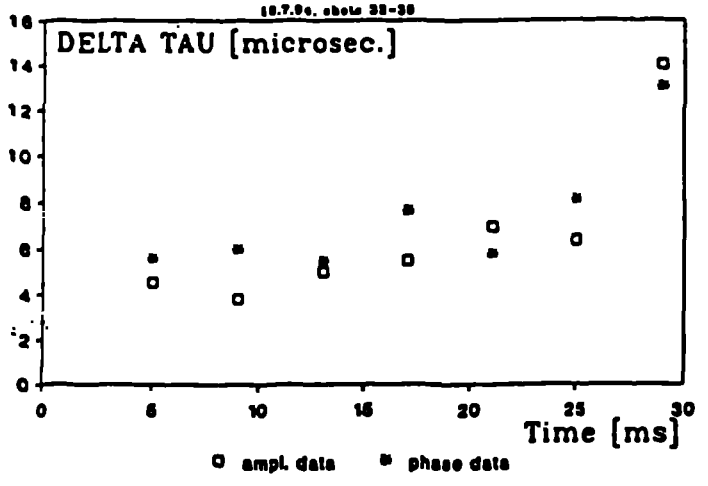

Figure 7a: The time evolution of $\Delta\tau$ parameter. The reflectometer has operated on the frequency 8.5GHz. $R_c = (8.2 - 8.4)cm$

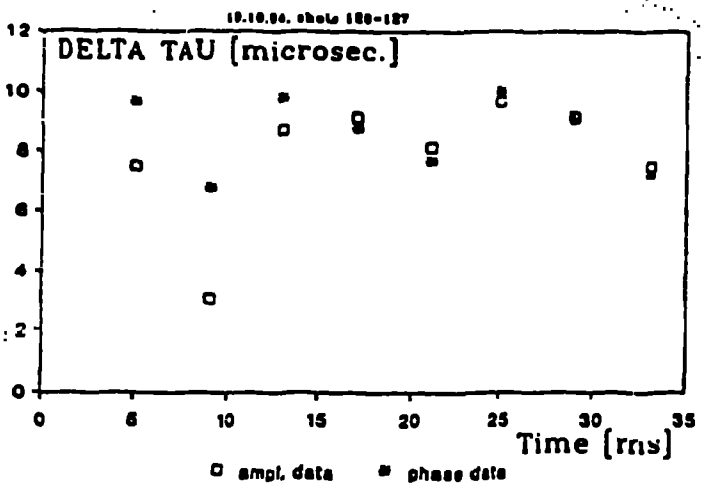

Figure 7b: The time evolution of $\Delta\tau$ parameter. The reflectometer has operated on the freguency 10.26GHz. $R_c = (7.2 - 8.0)cm$

The figures 7a and 7b show the time evolution of $\Delta\tau$ parameter for the two series of shots. The electron density of the first serie of shots (Fig.7a) was higher (Fig.5a) than the electorn density (Fig.5b) of the second serie of shots (Fig.7b). The density fluctuation spectra from two radially separated cutoff layers are shown in Fig.8a and Fig.8b.

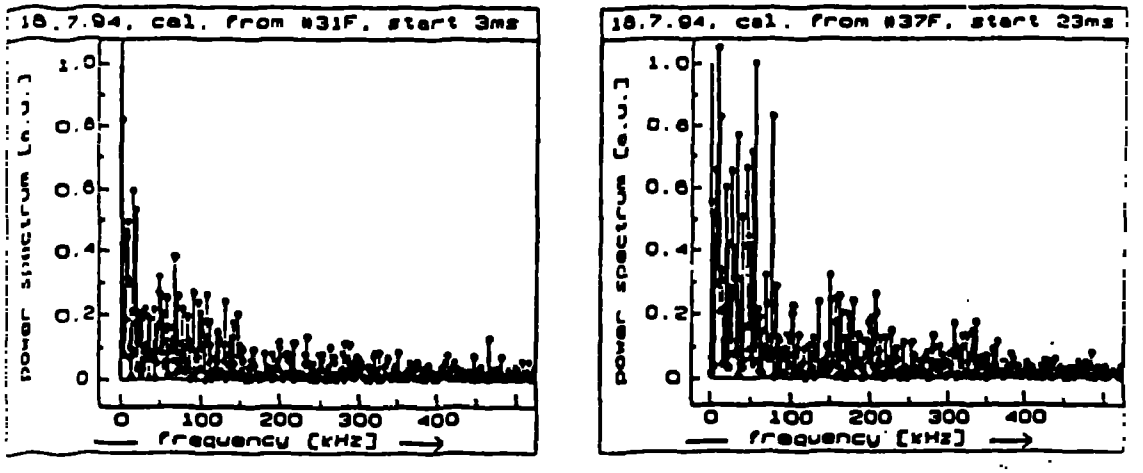

Figure 8a: The density fluctuation spectra at 3ms and 23ms from the start of discharge.

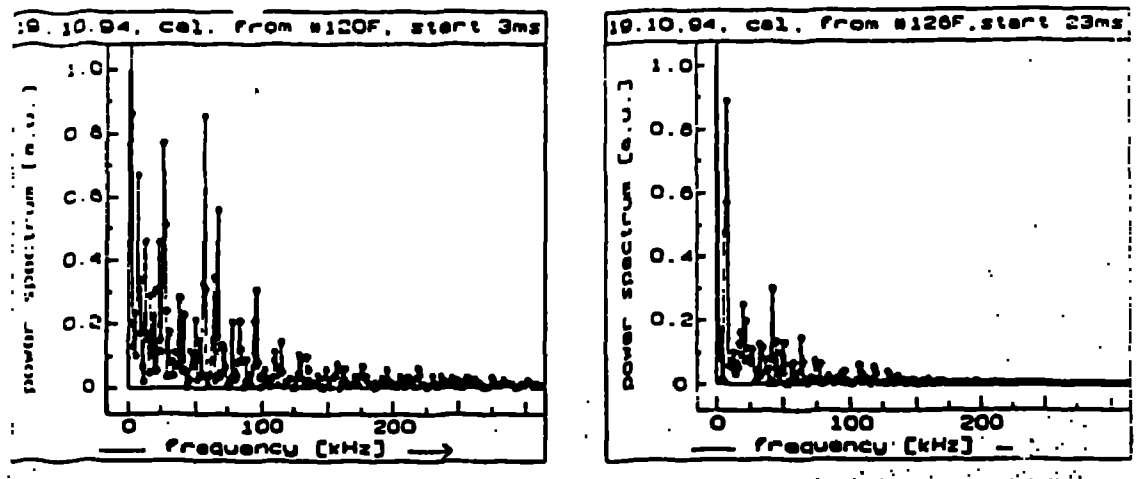

Figure 8b: The density fluctuation spectra at 3ms and 23ms from the start of discharge.

onclusion.

The report describes the analysing of first experimental data from sin-cosin reflectometer, which was used on the tokamak CASTOR for the measurement of the density fluctuations. The reflectometer is working on the two fix frequencies 8.5 GHz and 10.26 GHz, i.e. the fluctuations near to the plasma periphery are detected. The FFT and auto-correlation analysis was used to obtaining the frequency spectra of density fluctuation and the time evolution of $\Delta\tau$ parameter. From Fig.8a and Fig.8b is seem that the character of the spectra depends on used frequency (on the cutoff layer position). The content of higher frequencies in spectrum increases for the density fluctuations on plasma periphery. The correlation of fluctuations increases for the fluctuation at layers nearer to the plasma centrum.

cknowledgement.

I would like to express my gratitude to F. Žáček, L. Kryška and M. Člupek for their valuable discussions and comments.
The work was supported by the grant of GA ČR No: 202/93/1021.

eferences:

[1] Žáček F., Kletečka P.: "Test of 10GHz sin-cosin microwave reflectometer on CASTOR", IPPCZ-341.

[2] Kletečka P.: "Reflektometrie na tokamaku CASTOR", interní zpráva 2/94

[3] Žáček F., Stockel J., Kryška L., Badalec J., Jakubka K., Mlynář J., Magula P., Kletečka P., Svoboda V.: "Edge plasma turbulent characterictics on the CASTOR tokamak", 14th Internat. Conf. on Plasma Phys. and Controlled Nucl.Fus. Res., IAEA-CN-56/A-3-8, Oct. 1992, Wurzburg

[4] Hanson G.R.: "Microwave reflectometry on the advanced toroidal facility to measure density fluctuations and their radial correlation lengths"

[5] Čížek V.: " Diskrétní Fourierova transformace a její použití", matematický seminář SNTL. (1981)